

Title:

Polarization-Independent Switching With High Contrast
From A Liquid Crystal Polarization Grating

Authors:

Michael J. Escuti and W. Michael Jones

Affiliation:

North Carolina State University, Dept Electrical & Computer Engineering, Raleigh, NC (USA)

Presented At:

SID International Symposium, Seminar, and Exhibition, San Francisco, CA (June 4-9, 2006)

Citation:

M. J. Escuti and W. M. Jones, "Polarization-Independent Switching With High Contrast From A Liquid Crystal Polarization Grating," *SID Symposium Digest*, vol. 37, pp. 1443-1446, (2006).

Copyright 2006 Society For Information Display.

This paper was published in the SID Symposium Digest Vol. 37 and is made available as an electronic reprint. One print or electronic copy may be made for personal use only. Systematic or multiple reproduction, distribution to multiple locations via electronic or other means, duplication of any material in this paper for a fee or for commercial purposes, or modification of the content of this paper are prohibited.

39.4: Polarization-Independent Switching With High Contrast From A Liquid Crystal Polarization Grating

Michael J. Escuti¹ and W. Michael Jones

Dept of Electrical and Computer Engineering, North Carolina State University, Raleigh, NC, USA

Abstract

We report experimental results of a liquid crystal polarization grating (LCPG) modulating unpolarized light with high contrast for the first time. Striking results are observed: nearly ideal diffraction into the first orders at > 99%, contrast ratios of up to 600:1 for monochromatic light, switching times of ~ 2 ms for nematic LCs, and threshold voltage of 1.65 Vrms.

1. Introduction

Our objective is to develop a liquid crystal (LC) display element capable of modulating unpolarized light with high contrast, and to ultimately integrate it into a highly efficient portable projection display based on a light-emitting-diode (LED) light engine. A family of theoretically polarization-independent, binary, LC gratings was previously studied [1-3] but was plagued by the presence of domain boundary lines and random disclinations, were limited to very large grating periods, and did not achieve theoretical diffraction efficiencies (limiting contrast and brightness). Even the more recent improvements [4, 5] with polymer-wall LC gratings still manifest less than ideal efficiencies, diffract noticeably up to the 5th diffraction order, and are challenging to fabricate at periods on the order of 10s of μm . The central limitation in all of these approaches is the binary nature of the gratings.

Diffraction gratings that operate by periodically modulating the state of polarization of light passing through them are generally classed as “polarization gratings” [6, 7]. These are composed essentially of a periodically patterned optical anisotropy, and offer a unique opportunity to create switchable diffractive optics, particularly since it was observed early that PGs with 100% diffraction efficiency into the first order(s) could be achieved with a thin-grating regardless of input polarization.

Several research groups [8, 9] recognized that a continuous LC diffractive grating will have improved diffraction properties (over binary LC gratings), and that holography can be used to greatly simplify fabrication [10] and achieve smaller grating periods. Further theoretical studies by Zeldovich and coworkers [11, 12] identified compelling characteristics, including the potential to modulate unpolarized light with high contrast. Initial experimental results by Crawford and coworkers [10, 13] were promising, but were plagued by pervasive defects degrading their optical properties. Consequently, the maximum diffraction efficiency and switching contrast ratio was poor, and strong incoherent scattering outside of the diffraction orders was present [14].

We have overcome these deficiencies by carefully balancing the choice of LC and photo-alignment materials with cell geometry to experimentally realize ideal polarization gratings. As far as we are aware, this is the first experimental success at realizing the anticipated properties of LCPGs with high quality.

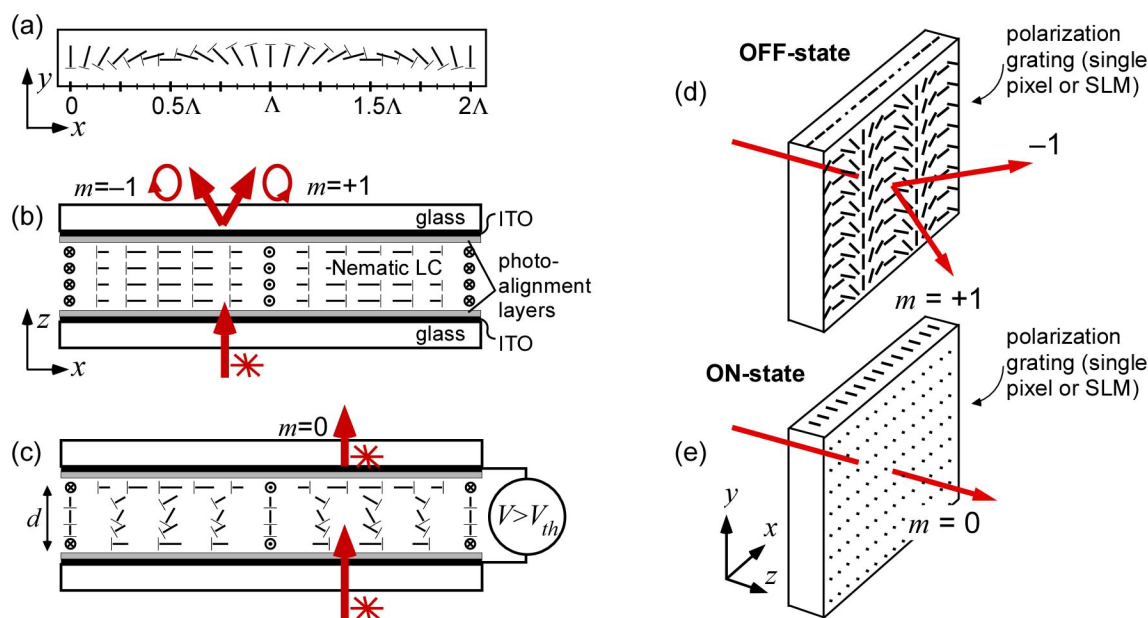


Figure 1 – The liquid crystal polarization grating (LCPG): (a) Basic geometry (top view); (b) Basic geometry (side view) and illustrated diffraction behavior when $\Delta nd = \lambda/2$ with zero applied voltage; (c) Nematic texture and diffraction behavior when the applied voltage exceeds V_{th} ; Operational illustrations of the (d) OFF-state and (e) ON-state.

¹ Preferred email contact: mjescuti@ncsu.edu

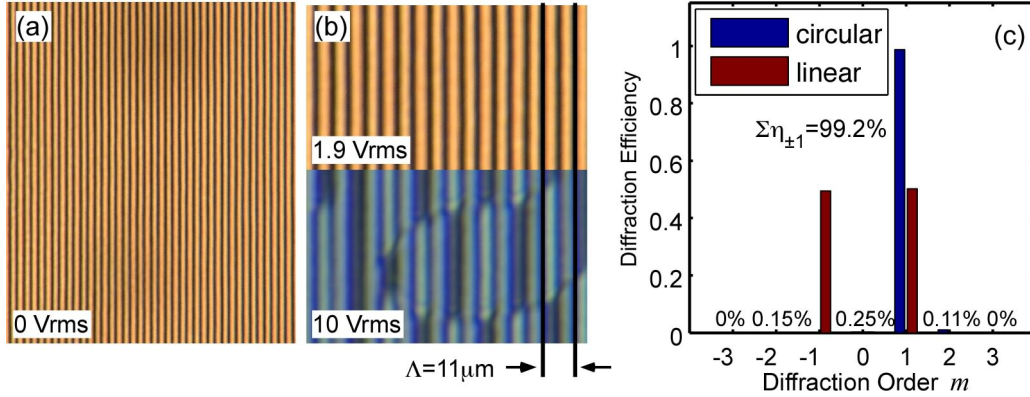


Figure 2 – (a) The LCPG between crossed polarizers; (b) Higher magnification view; (c) Measured diffraction efficiencies at Vrms = 1.9V for linear and circular input polarized light that are remarkably close to theoretical prediction.

2. LC Polarization Grating Properties

The essence of the LCPG is an in-plane, uniaxial birefringence that varies with position, $\mathbf{n}(x) = [\sin(\pi x/\Lambda), \cos(\pi x/\Lambda), 0]$, as shown in Figure 1. From the elastic continuum point of view, this LC configuration should be viable as long as the thickness d of the LC layer is below a critical thickness [15]. In order to find a concise summary of the optical properties of this grating, we employ similar reasoning as in Refs. [6, 7]. We start with the paraxial approximation for an infinite grating and express the (far-field) electric field \mathbf{D}_m for each diffraction order m transformed from the (near-field) output of the diffraction grating $\mathbf{T}(x)\mathbf{E}_m$:

$$\mathbf{D}_m = \frac{1}{\Lambda} \int_0^\Lambda \mathbf{T}(x)\mathbf{E}_m \exp\{-i2\pi mx/\Lambda\} dx, \quad (1)$$

where Λ is half of the nematic period as defined in Figure 1(a), $\mathbf{T}(x) = \exp\{i\pi\Delta\mathbf{n}(x)d/\lambda\}$ is the spatially-varying 2×2 Jones transfer matrix of the PG, $\Delta\mathbf{n}(x)$ is the birefringence tensor describing the local uniaxial anisotropy, and \mathbf{E}_m is the complex Jones vector of the input lightwave. Neglecting the absolute phase,

$$\mathbf{T}(x) = \cos\zeta \mathbf{I} + i \sin\zeta \begin{bmatrix} \sin\delta(x) & \cos\delta(x) \\ \cos\delta(x) & -\sin\delta(x) \end{bmatrix}, \quad (2)$$

where $\zeta = \pi\Delta nd/\lambda$, Δn is the birefringence, d is the thickness, \mathbf{I} is the identity matrix, and $\delta(x) = 2\pi x/\Lambda$.

The integral in Eq. (1) can be analytically evaluated to find

$$\mathbf{D}_0 = (\cos\zeta)\mathbf{E}_m \quad \text{and} \quad \mathbf{D}_{\pm 1} = \frac{\sin\zeta}{2} \begin{bmatrix} \mp i & 1 \\ 1 & \pm i \end{bmatrix} \mathbf{E}_m, \quad (3)$$

and $\mathbf{D}_m = 0$ for all $m \geq 2$. Since the diffraction efficiency is defined as the ratio of output to input intensity ($\eta_m = |\mathbf{D}_m|^2/|\mathbf{E}_m|^2$), we find that the diffraction efficiency of the LCPG is

$$\eta_0 = \cos^2\left(\frac{\pi\Delta nd}{\lambda}\right) \quad \text{and} \quad \eta_{\pm 1} = \frac{1}{2} [1 \mp S'_3] \sin^2\left(\frac{\pi\Delta nd}{\lambda}\right). \quad (4)$$

where η_m is the diffraction efficiency of the m^{th} -order, λ is the wavelength of incident light, and $S'_3 = S_3/S_0$ is the normalized Stokes parameter corresponding to ellipticity of incident light. We assume normal incidence and a thin grating ($Q = 2\pi\lambda d/n_0\Lambda^2 < 1$).

Several notable features are summarized in Eq. (1) with relevance to switchable LCPG modulators:

1. the zero order is polarization insensitive and reaches a minimum (0%) when the retardation is halfwave ($\Delta nd = \lambda/2$);

2. the first orders show maximum diffraction (up to 100%) when $\Delta nd = \lambda/2$;
3. diffraction between the $\pm 1^{\text{st}}$ -orders is polarization sensitive.

Electro-optic switching occurs in the LCPG as an applied field re-orientates the nematic director out of plane, decreasing the effective retardation (as with a uniform planar tunable LC waveplate), and allowing energy to couple from the ± 1 -orders into the 0^{th} -order (as in Figure 1(d) and (e)).

It can also be shown that $\Lambda = \lambda_{\text{rec}}/(2\sin\theta)$ where λ_{rec} is the hologram recording wavelength and θ is half the angle between the recording beams. Note that this grating follows the normal diffraction equation $m\lambda/\Lambda = \sin\theta_{\text{in}} + \sin\theta_{\text{m}}$ even though Λ is defined as half the period of the nematic director.

3. Experiment

The LCPG is fabricated as follows: first, ITO-coated substrates must be coated with a UV-sensitive photo-alignment layer [16] and the LC cell with a fixed spacing d must be assembled. Second, the cell is exposed to a UV polarization hologram (with superimposed, orthogonal circularly polarized beams leading to a linearly polarized standing optical wave). Third, this cell is filled with a nematic LC (preferably within its isotropic state). The simple holographic setup is explicitly illustrated in Refs. [6, 10].

Previous experimental work with LCPGs [10, 13] led to less-than ideal LC alignment rife with defects. We have overcome this through two primary avenues: designing cell geometry in view of the critical thickness [12, 15], and by extensive materials optimization (of both the LC and photo-alignment layers).

The following fabrication parameters were used for the results reported here. Standard ITO-glass was assembled to achieve a 2 μm cell thickness. We used the photo-alignment layer [16] ROP201 (ROLIC, with standard recommend processing) and the liquid crystal MLC-6080 (MERCK, $\Delta n = 0.202$, $T_{\text{NI}} = 95^\circ\text{C}$). A HeCd laser (325 nm) delivering a dose of $\sim 300 \text{ mJ/cm}^2$ with orthogonal circularly polarized beams was used to expose a surface alignment pattern with a grating period of $\Lambda = 11 \mu\text{m}$. Filling of the LC was done on a hotplate at 115°C and annealed on another hotplate at 90°C for 2 min.

We determine the diffraction efficiency of the holographic grating in the normal way: $\eta_m = I_m / I_{\text{REF}\#1}$, where I_m is the measured intensity of the m^{th} transmitted diffraction order, and where $I_{\text{REF}\#1}$ is a reference intensity for an ITO-glass cell filled with a solvent.

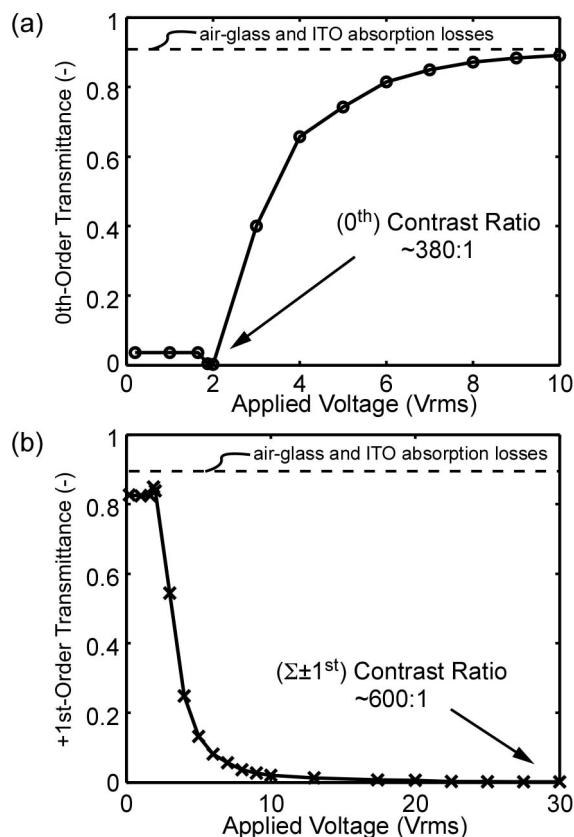


Figure 3 – LCPG transmission vs. voltage characteristics, measured with a HeNe laser input (633 nm): (a) zero order and (b) first order response. Note that both η_0 and $\Sigma\eta_{\pm 1}$ were experimentally found to be polarization independent.

This isolates effect of the hologram in order to compare experimental data directly with Eq. (4). A slightly different measure, transmittance (T), is defined as $T = I_{\text{MOD}} / I_{\text{REF\#2}}$, where I_{MOD} is the modulated intensity of the LCPG and $I_{\text{REF\#2}}$ is reference intensity with the LCPG removed. This measure includes the effect of the cell reflections and any absorption. All electro-optic measurements were done with a 4 kHz square wave.

4. Results

We generally find excellent agreement between our initial experimental results of transmission spectra and Eq. (4). The fabricated samples are free of defects over very large areas, as seen in Figure 2(a). A magnified view of the LC texture between crossed polarizers is shown in Figure 2(b), which shows a sinusoidal grayscale pattern as is expected (since the azimuthal angle of $\mathbf{n}(x)$ is proportional to x). With small voltages applied, a uniform texture is seen, while at voltages $\gg V_{th}$, the grating structure becomes much darker and disclination lines appear over very large length scales (Figure 2(c)). These appear at first glance to be the standard domain wall boundaries appearing in LC layers that have nearly zero pretilt angle (as we have here).

4.1 Static Electro-Optical Response

Most remarkably, the diffraction of a HeNe (633nm) laser is maintained almost completely within the 0th- and $\pm 1^{\text{st}}$ -orders regardless of voltage, as shown in Figure 2(c). It is completely insensitive to the direction of linearly polarized light ($S_3^0 = 0$), but

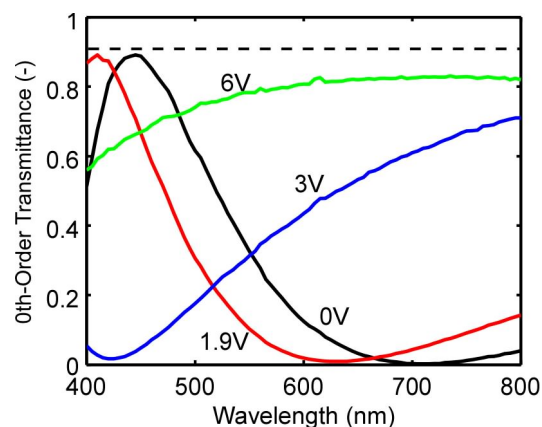


Figure 4 – LCPG transmission spectra for several applied voltages. Notice that the transmission minimum shifts to smaller wavelengths. ($\Lambda = 11 \mu\text{m}$ and $d = 2.0 \mu\text{m}$)

will couple between the +1 and -1 orders when the light is elliptically polarized ($S_3^0 \neq 0$). In extreme case of incident light with circular polarization, we find that the diffraction into the +1 order is 99.2%. Very little incoherent scattering ($< 0.3\%$ for red light) is routinely observed.

Basic switching behavior is shown in Figure 3 for HeNe (633 nm) laser light. As expected, a voltage threshold exists [10, 15], and was $V_{th} = 1.65$ V for this sample. The transmittance vs. voltage revealed a contrast ratio of $\sim 380:1$ for the 0th-order (Figure 3(a)) and a maximum that approached the air-glass limit even at ≤ 10 V. The transmittance curve for the first order revealed a higher contrast ratio of 600:1, but required higher voltages (~ 30 V).

Transmission spectra at several applied voltages with unpolarized input light were acquired with a spectrophotometer (Figure 4). For this measurement, we blocked the ± 1 orders with an iris and allowed only the zero order to be observed by the spectrophotometer. The applied voltage shifts the entire spectrum toward the blue, suggesting that the applied voltage acts by effectively reducing the birefringence. The minimum transmittance remains low for all voltages, with only a small degradation at shorter wavelengths. We are hopeful that this can be improved by producing samples with an increased angle between the diffraction orders (by reducing Λ below $\sim 7 \mu\text{m}$). We stress that the data in Figures 3 and 4 are “real” transmittance values, where the baseline was taken with the LCPG removed and without further normalization, biasing, or scaling.

4.2 Dynamic Response

The full-contrast switching times of the 0th-order intensity were measured with the HeNe laser and a modulated drive signal. Figure 4(a) shows a screenshot of the LCPG responding to a 10 V (RMS) square wave. A summary of the 10%-90% rise and fall times vs. applied voltage is shown in Figure 4(b). Somewhat surprisingly, the switching times are all on the order of ~ 2 ms, a phenomenon that has been verified across several samples.

5. Discussion

Any display element that can modulate unpolarized light with high contrast can immediately offer superior system-power efficiency and/or brightness. When used in combination with a field-sequential color light engine, overall efficiency will be enhanced over current conventional LC projector designs. The LCPG

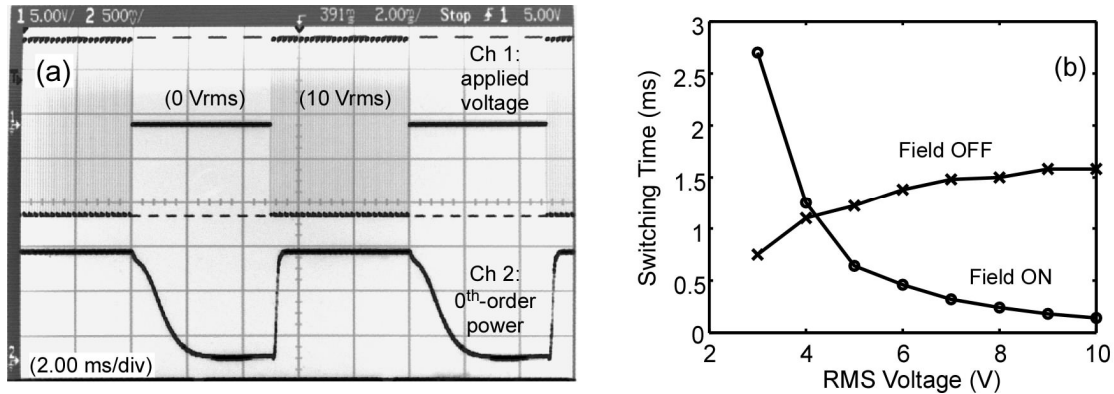


Figure 5 – Time-dependent diffraction of LCPG: (a) Oscilloscope screenshot of applied voltage and 0th-order power, measured with a HeNe laser input (633 nm); (b) Full contrast switching times. ($\Lambda = 11 \mu\text{m}$ and $d = 2.0 \mu\text{m}$)

described here has shown high contrast and high brightness and could finally enable feasible “pocket” projectors (small battery powered mobile data projectors) and integrated data projectors (e.g. within laptops). A study reporting our early results related to this effort [17] shows that reasonable contrast ratios of ~100:1 for all colors are possible when the LCPG is arranged with a LED light engine and projection optics. Additionally, we have numerically modeled the minimum pixel size of a spatial-light-modulator (SLM) based on the LCPG [15], and found it to be approximately 2-4 times the grating period, which suggests that minimum pixel sizes could be as low as ~10-20 μm .

The primary limit on the maximum brightness of this modulator element are the losses from the air-glass interfaces and from the ITO absorption (which is the case for all LC displays can be improved with anti-reflection coatings).

Several advantages of the LCPG are apparent as compared to the most extensively studied type of LC diffraction gratings: Holographic-Polymer Dispersed Liquid Crystals (H-PDLCs) [18-20]. Approximately equivalent high diffraction efficiencies can be achieved, but the LCPG offers with substantially lower drive voltages and reduced scattering. Furthermore, the LCPG gratings are inherently wavelength-tunable. However, the minimum switching times in the LCPG are so far not as small as with H-PDLCs, the maximum diffraction angle is comparably lower, and the LCPG approach cannot record volume holographic patterns.

6. Conclusions

We have experimentally demonstrated polarization-independent switching with high contrast at modest drive voltages using the LCPG. For monochromatic light, the contrast ratios have reached 600:1, and the total switching times with a nematic LC are ~2 ms. Very low scattering is observed, and almost all diffracted light (~99.45%) appears in the 0th- and $\pm 1^{\text{st}}$ -orders. The holographic fabrication process is relatively simple and fast, but high quality LCPG alignment is only possible when the cell thickness is less than the critical thickness. We are persuaded that the LCPG shows great promise as the active element for compact, ultra-portable projection displays.

7. Acknowledgements

The authors gratefully acknowledge the support of the National Science Foundation through a STTR Phase 1 grant (OII 0539552), in partnership with Southeast TechInventures Inc. and

ImagineOptix Corp. MJE also thanks Dick Broer, Cees Bastiaansen, Carlos Sanchez, and Chongchang Mao for many fruitful technical discussions supporting this research.

8. References

- [1] J. Chen *et al.*, *Appl. Phys. Lett.*, vol. **67**, pp. 2588-2590 (1995).
- [2] C. M. Titus, P. J. Bos, *Appl. Phys. Lett.*, vol. **71**, pp. 2239-2241 (1997).
- [3] M. Honma, T. Nose, *Appl. Opt.*, vol. **43**, pp. 5193-5197 (2004).
- [4] Y. Zhang *et al.*, *SID Digest*, vol. **36**, pp. 1178-1181 (2005).
- [5] B. Wang, X. Wang, P. J. Bos, *J. Opt. Soc. Amer. A*, vol. **21**, pp. 1066-1072 (2004).
- [6] L. Nikolova, T. Todorov, *Optica Acta*, vol. **31**, pp. 579-588 (1984).
- [7] J. Tervo, J. Turunen, *Opt. Lett.*, vol. **25**, pp. 785-786 (2000).
- [8] H. Sarkissian *et al.*, *SPIE Optics in the Southeast Conference Orlando FL, PSE-02*, 2003.
- [9] J. Tervo *et al.*, *J. Opt. Soc. Amer. A*, vol. **20**, pp. 282-289 (2003).
- [10] J. Eakin *et al.*, *Appl. Phys. Lett.*, vol. **85**, pp. 1671-1673 (2004).
- [11] H. Sarkissian *et al.*, *Storming Media Report*, **A000824**, (2004).
- [12] H. Sarkissian *et al.*, *Proc. of CLEO/QELS Baltimore MD*, poster JThe12 (2005).
- [13] G. P. Crawford *et al.*, *J. Appl. Phys.*, vol. **98**, pp. 123102 (2005).
- [14] (personal communication with G. P. Crawford).
- [15] C. Oh, R. Komanduri, M. J. Escuti, *SID Digest*, vol. **37**, pp. P167 (2006).
- [16] M. Schadt, H. Seiberle, A. Schuster, *Nature*, vol. **381**, pp. 212-215 (1996).
- [17] W. M. Jones, B. L. Conover, M. J. Escuti, *SID Digest*, vol. **37**, pp. P209 (2006).
- [18] T. J. Bunning *et al.*, *Annu. Rev. Mater. Sci.*, vol. **30**, pp. 83-115 (2000).
- [19] G. P. Crawford, *Opt. Photon. News*, vol. **14**, pp. 54-59 (2003).
- [20] Y. H. Cho *et al.*, *Chem. Mater.*, vol. **17**, pp. 6263-6271 (2005).